

# An online battery–state of charge estimation method using the varying forgetting factor recursive least square-unscented Kalman filter algorithm on electric vehicles

Nguyen Thi Diep<sup>1</sup>, Nguyen Kien Trung<sup>2</sup>

<sup>1</sup>Faculty of Control and Automation, Electric Power University, Hanoi, Vietnam

<sup>2</sup>School of Electrical and Electronic Engineering, Hanoi University of Science and Technology, Hanoi, Vietnam

## Article Info

### Article history:

Received Dec 12, 2023

Revised Feb 19, 2024

Accepted Feb 20, 2024

### Keywords:

Battery management system

Electric vehicle

Lithium-ion battery

State of charge estimation

Unscented Kalman filter

## ABSTRACT

Accurate and fast estimation of the state of charge is important for the battery management system of electric vehicles. This paper proposes a method to estimate the state of charge of Lithium-ion batteries by the variable forgetting factor recursive least square (VFFRLS) – unscented Kalman filter (UKF) algorithm in real-time without the off-line battery testing data. Since the state observation requires an accurate model, an equivalent circuit model was constructed. Then, the VFFRLS algorithm is used to identify online the battery model parameters based on voltage and current measurements. An advantage of this algorithm is that it requires less initial information and shorter identification time than offline parameter identification. After the model parameters are well identified, the unscented Kalman filter estimates the state of charge and minimizes noise characteristics and uncertainty in the parameter identification process. The VFFRLS algorithm applied in this paper has shown a good result with the model output error of less than 1%, and the identification achieves real-time response. The state of charge obtained by the UKF algorithm has shown satisfactory estimation results with fast convergence speed and small errors. The UKF filter provides the results with a 1.5% error from the reference and converges after 10 cycles.

*This is an open access article under the [CC BY-SA](https://creativecommons.org/licenses/by-sa/4.0/) license.*



## Corresponding Author:

Nguyen Kien Trung

School of Electrical and Electronic Engineering, Hanoi University of Science and Technology

No 1 Dai Co Viet, Hanoi, Vietnam

Email: trung.nguyenkien1@hust.edu.vn

## 1. INTRODUCTION

Currently, electric vehicles (EVs) are increasingly popular because they are environmentally friendly [1]. The performance of EVs is highly dependent on the energy storage system in the vehicle. Among current energy storage technologies, Lithium-ion batteries (LIBs) are preferred because they have many outstanding advantages as high energy density, long life cycle, and low self-discharge. However, LIBs still have disadvantages such as sensitivity to the short discharge of the output circuit, sensitivity to overheating when charging, and easily causing explosions when left unchecked [2]–[4]. Therefore, a battery management system (BMS) is needed for LIBs on EVs. The functions of the BMS system include charging and discharging control, battery cell balancing, battery temperature control, and estimating the state of charge (SOC). The SOC estimation is a crucial function of BMS, defining the battery's remaining capacity as a percentage of its maximum capacity. SOC is a quantity that can only be estimated and cannot be measured directly [5]–[10].

The literature suggests that SOC estimation methods include coulomb counting, data-driven, and model-based methods. While the coulomb counting method is simple to implement in BMS, it has a higher possibility of SOC estimation errors due to cumulative measurement errors [11], [12]. Data-driven methods need a lot of training data set under different operating conditions and take a long time to develop [13], [14]. Currently, model-based methods are extensively employed for SOC estimation due to their high accuracy. Several algorithms have been developed for model-based SOC estimation as the Kalman filter and its derivative algorithm method. Kalman filter algorithm can automatically adjust the original SOC error online and reduce the measured noise impact [15]–[18]. However, the error resulting from the linearization and calculation of the Jacobian matrix causes the accuracy of the Kalman filter algorithm to decrease [19]. The unscented Kalman filter (UKF) algorithm, built upon the unscented transform, is developed to solve the above problems [20]–[23]. The UKF algorithm provides an approximation of the probability density distribution for a nonlinear function. Due to the advantages of the model-based estimation method, including high accuracy and low computational complexity, the UKF algorithm has been selected for use in this paper.

Accurate determination of pin model parameters is crucial in model-based SOC estimation methods. Typically, battery model parameters are determined offline based on data collected in the laboratory. To acquire this testing data, various testing procedures like the open circuit voltage test, the hybrid pulse power characterization test, and others must be performed, requiring the establishment of complex battery test workbenches, which can be costly and time-consuming. Moreover, the data obtained may only be suitable for the particular battery under test and possibly limited to a specific state of the battery. Over time, as the battery is used extensively, its parameters may change, taking the SOC estimation error [24]–[26]. To solve this problem, a variable forgetting factor recursive least square (VFFRLS) algorithm is proposed to identify the parameters of the battery model in real-time. The VFFRLS algorithm is an adaptive variant of the conventional recursive least square algorithm that added a varying forgetting factor. In this way, batteries can be directly integrated into EVs, and battery model parameters can be obtained automatically [27].

This paper proposes an online battery SOC estimation method using the VFFRLS-UKF algorithm on EVs. First, battery parameters are identified online based on the VFFRLS algorithm. Then, the UKF algorithm is used to estimate the SOC and minimize noise characteristics and uncertainty in the parameter identification process. Finally, the hardware implementation of the algorithm is detailed, and the experimental results are analyzed and evaluated.

## 2. BATTERY PARAMETER IDENTIFICATION

### 2.1. Equivalent circuit model of Lithium-ion battery

The equivalent circuit model of a LIB is expressed in Figure 1. The circuit contains the open circuit voltage (OCV)  $U_{OCV}$ , the battery's internal resistance  $R_0$  connects in series with  $R_1 - C_1$  branch that demonstrates the dynamic properties of the LIB.

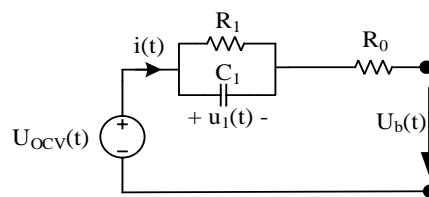


Figure 1. Battery equivalent circuit model

The Thevenin model is built to determine the components of the circuit in a continuous domain:

$$\begin{cases} sU_1(s) = \frac{I(s)}{C_1} - \frac{U_1(s)}{R_1 C_1} \\ U_b(s) = U_{OCV}(s) - U_1(s) - R_0 I(s) \end{cases} \quad (1)$$

The difference between the output voltage and open-circuit voltage:

$$U_b(s) - U_{OCV}(s) = -I(s) \left( R_0 + \frac{R_1}{1 + R_1 C_1 s} \right) \quad (2)$$

The transfer function is represented as in (3).

$$G(s) = \frac{U_b(s) - U_{OCV}(s)}{I(s)} = \frac{E_L(s)}{I(s)} = -\frac{R_0 + R_1 + R_0 R_1 C_1 s}{1 + R_1 C_1 s} \quad (3)$$

where  $E_L(s) = U_b(s) - U_{OCV}(s)$ .

Convert to the discretized domain using the Tustin method. Replace  $s = \frac{2}{T} \frac{1-z^{-1}}{1+z^{-1}}$ , obtain:

$$G(z^{-1}) = \frac{a_2 + a_3 z^{-1}}{1 - a_1 z^{-1}} \quad (4)$$

where  $a_1 = -\frac{T-2R_1C_1}{T+2R_1C_1}$ ;  $a_2 = -\frac{R_0T+R_1T+2R_0R_1C_1}{T+2R_1C_1}$ ;  $a_3 = -\frac{R_0T+R_1T-2R_0R_1C_1}{T+2R_1C_1}$ . Equation (3) and (4) is rewritten after discretization, with  $k = 1, 2, 3 \dots$

$$E_L(k) = a_1 E_L(k-1) + a_2 I(k) + a_3 I(k-1) \quad (5)$$

The open-circuit voltage value is affected by the SOC in working temperature ( $Te$ ) and aging conditions of battery  $H$ , which is described by (6).

$$\frac{dU_{OCV}}{dt} = \frac{\partial U_{OCV}}{\partial SOC} \frac{\partial SOC}{\partial t} + \frac{\partial U_{OCV}}{\partial Te} \frac{\partial Te}{\partial t} + \frac{\partial U_{OCV}}{\partial H} \frac{\partial H}{\partial t} \quad (6)$$

Since the sample time is much smaller than the full discharge or full charge time of the battery, in one sample period it is possible to consider the remaining capacity (SOC) unchanged or  $\frac{\partial SOC}{\partial t} \approx 0$ . The rate of temperature change is almost constant over a small sample period,  $\frac{\partial Te}{\partial t} \approx 0$ . In a short period, the aging of the battery is negligible,  $\frac{\partial H}{\partial t} \approx 0$ . Equation (6) is rewritten as (7).

$$\frac{dU_{OCV}}{dt} = \frac{U_{OCV}(k) - U_{OCV}(k-1)}{T} \approx 0 \quad (7)$$

$$\Delta U_{OCV}(k) = U_{OCV}(k) - U_{OCV}(k-1) \approx 0 \quad (8)$$

The voltage between two battery terminals is defined as follows using (5) and (8):

$$U_b(k) = (1 - a_1)U_{OCV}(k) + a_1 U_b(k-1) + a_2 I(k) + a_3 I(k-1) = \phi(k)\theta(k) \quad (9)$$

$$\text{where: } \phi(k) = [1, U_b(k-1), I(k), I(k-1)] \quad (10)$$

$$\theta(k) = [(1 - a_1)U_{OCV}(k), a_1, a_2, a_3]^T \quad (11)$$

Vectors  $\theta$  can be determined by a series of recursive formulas to be able to calculate the values  $a_1, a_2, a_3$  and thereby determine the  $R_0, C_1, R_1$  values of the LIB model.

## 2.2. Online parameters identification of battery using VFFRLS

In this paper, the VFFRLS algorithm was combined with blocking conditions to estimate online the parameters of the LIB model. These blocking conditions are used to prevent the estimation algorithm from calculating non-physical parameters. The VFFRLS algorithm is an adaptive variant of the conventional recursive least square (RLS) algorithm. VFFRLS proposes in this study to solve this problem by adding a varying forgetting factor (VFF). The model parameter estimations are continually updated during the sampling interval by combining the quantity measured at time  $k$  and the previous estimates at the time  $(k-1)$ . The LIB model above can be presented as follows. The estimated output value of the LIB model is represented:

$$y(k) = \phi(k)\theta(k) + e(k) \quad (12)$$

The error between the output voltage value of the model and the actual measurement value at time  $k$ :

$$e(k) = U_b(k) - \phi(k)\hat{\theta}(k-1) \quad (13)$$

In RLS algorithms in general, the parameter vector  $\theta_k$  is the sum of the old value  $\theta_{k-1}$  and the specified component  $K_k e_k$ . In which,  $K_k$  is the corrective coefficient calculated to minimize the target function:

$J_k = E(\lambda^k e_k^T e_k) = Tr P_k$ . The target function  $J_k$  is the trace of the variance matrix  $P_k$ . Calculate the gain  $K_k$  so that it  $J_k$  is the smallest at each update step.

- Gain of VFFRLS:

$$K(k) = \frac{P(k-1)\phi^T(k)}{\lambda(k-1) + \phi^T(k)P(k-1)\phi(k)} \tag{14}$$

- The model's estimated parameter vector:

$$\hat{\theta}(k) = \hat{\theta}(k-1) + K(k)e(k) \tag{15}$$

- Update the covariance of estimated and actual values:

$$P(k) = \frac{P(k-1) - K(k)\phi^T(k)P(k-1)}{\lambda(k-1)} \tag{16}$$

- Update the VFF forget factor:

$$\lambda(k) = 1 - \frac{e^2(k)}{1 + K^T(k)P(k)K(k)} \tag{17}$$

where  $\hat{\theta}(k)$  is the estimate of vector  $\theta(k)$ ;  $e(k)$  is the estimation error of the terminal voltage  $U_b(k)$ . The idea of the forgetting factor  $\lambda(k)$  can be easily noticed in (17). When the system changes suddenly, the error of model output values, then  $\lambda(k)$  decreases. In other words, the weight of the previously estimated values decreases, the weight of the new measurement cycle (when the system has just changed) increases, and the parameters update results respond quickly to such changes in the system. On the other hand, when the dynamics of the system slow down, or the system has reached a new working point, this time the estimation error decreases, and  $\lambda(k)$  increases close to 1. Then, the algorithm returns to the form of the normal RLS, ensuring stability in the estimation process. The flow chart of the VFFRLS algorithm is presented in Figure 2. After determining the lithium battery model parameters, the next step is to estimate SOC using the UKF method.

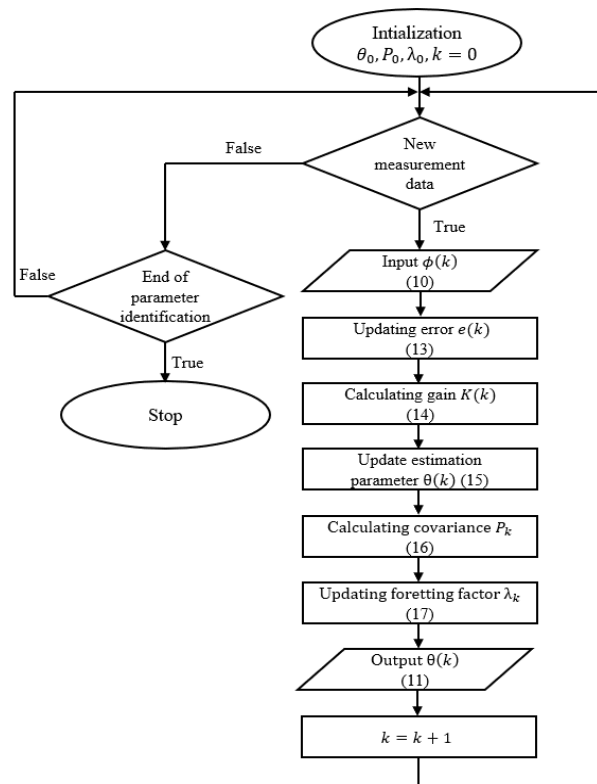


Figure 2. The VFFRLS algorithm flowchart

### 3. UNSCENTED KALMAN FILTER FOR SOC ESTIMATION

The state equations of the battery model shown in Figure 1 are presented as (18).

$$\begin{bmatrix} SOC_k \\ U_{1,k} \end{bmatrix} = \begin{bmatrix} 1 & 0 \\ 0 & \exp\left(-\frac{\Delta t}{\tau}\right) \end{bmatrix} \begin{bmatrix} SOC_k \\ U_{1,k} \end{bmatrix} + \begin{bmatrix} -\frac{\eta \Delta t}{Q_c} \\ R_1 \left(1 - \exp\left(-\frac{\Delta t}{\tau}\right)\right) \end{bmatrix} I_{k-1} + \begin{bmatrix} W_{1,k-1} \\ W_{2,k-1} \end{bmatrix} \quad (18)$$

$$U_{b,k} = U_{OCV}(SOC_k) - U_{1,k} - R_0 I_k + v_k \quad (19)$$

where  $U_{OCV}$  is a function dependent on the SOC and SOC achieved by the Coulomb counting method,  $\tau = R_1 C_1$ ,  $\eta$  is the discharge coefficient of the battery. Set the state variable  $x_k = [SOC_k, U_{1,k}]^T$ , the input variable  $u_k = I_k$ .  $w_k = [w_1(k) \ w_2(k)]^T$  and  $v_k$  are correspondingly the process noise and measurement noise (both independent white noises subject to Gaussian law) in which their covariances  $Q_k$  and  $R_k$ . The general state equation system is described as (20).

$$\begin{cases} x_k = f(x_{k-1}, u_{k-1}) + w_{k-1} \\ y_k = h(x_k, u_k) + v_k \end{cases} \quad (20)$$

The estimation process by UKF consists of two steps time update and measurement update. UKF is initialized as (21).

$$\begin{aligned} \hat{x}_0^+ &= E(x_0) \\ P_0^+ &= E[(x_0 - \hat{x}_0^+)(x_0 - \hat{x}_0^+)^T] \end{aligned} \quad (21)$$

#### 3.1. Time update

Select sigma points for unscented transformation:

$$\begin{aligned} x^{(i)} &= \bar{x} + \tilde{x}^{(i)}, & i &= 1, 2, \dots, 2n \\ \tilde{x}^{(i)} &= \left(\sqrt{nP_{k-1}^+}\right)_i^T, & i &= 1, 2, \dots, n \\ \tilde{x}^{(n+i)} &= -\left(\sqrt{nP_{k-1}^+}\right)_i^T, & i &= 1, 2, \dots, n \end{aligned} \quad (22)$$

Unscented transformation of sigma points through the transition function:

$$\hat{x}_k^{(i)} = f(\hat{x}_{k-1}^{(i)}, u_k) \quad (23)$$

Estimation of priori state:

$$\hat{x}_k^- = \frac{1}{2n} \sum_{i=1}^{2n} \hat{x}_k^{(i)} \quad (24)$$

Estimation of priori variance with process noise is considered:

$$P_k^- = \frac{1}{2n} \sum_{i=1}^{2n} (\hat{x}_k^{(i)} - \hat{x}_k^-)(\hat{x}_k^{(i)} - \hat{x}_k^-)^T + Q_{k-1} \quad (25)$$

#### 3.2. Measurement updates

Selecting sigma points of priori state based on  $P_k^-$ :

$$\begin{aligned} x^{(i)} &= \bar{x} + \tilde{x}^{(i)}, & i &= 1, 2, \dots, 2n \\ \tilde{x}^{(i)} &= \left(\sqrt{nP_k^-}\right)_i^T, & i &= 1, 2, \dots, n \\ \tilde{x}^{(n+i)} &= -\left(\sqrt{nP_k^-}\right)_i^T, & i &= 1, 2, \dots, n \end{aligned} \quad (26)$$

Unscented transformation of sigma points through the output function:

$$\hat{y}_k^{(i)} = h(\hat{x}_k^{(i)}, u_k) \quad (27)$$

Estimated output value

$$\hat{y}_k = \frac{1}{2n} \sum_{i=1}^{2n} \hat{y}_k^{(i)} \tag{28}$$

Estimated output covariance:

$$P_y = \frac{1}{2n} \sum_{i=1}^{2n} (\hat{y}_k^{(i)} - \hat{y}_k)(\hat{y}_k^{(i)} - \hat{y}_k)^T + R_k \tag{29}$$

Estimated priori covariance and output:

$$P_{xy} = \frac{1}{2n} \sum_{i=1}^{2n} (\hat{x}_k^{(i)} - \hat{x}_k^-)(\hat{y}_k^{(i)} - \hat{y}_k)^T \tag{30}$$

Posterior updates

$$\begin{aligned} K_k &= P_{xy} P_y^{-1} \\ \hat{x}_k^+ &= \hat{x}_k^- + K_k (y_k - \hat{y}_k) \\ P_k^+ &= P_k^- - K_k P_y K_k^T \end{aligned} \tag{31}$$

Note that the state space model of the battery includes two states; in (26)-(31), n equals 2. By taking these steps, the SOC value is obtained from the state estimation. Figure 3 presents the SOC estimation flowchart.

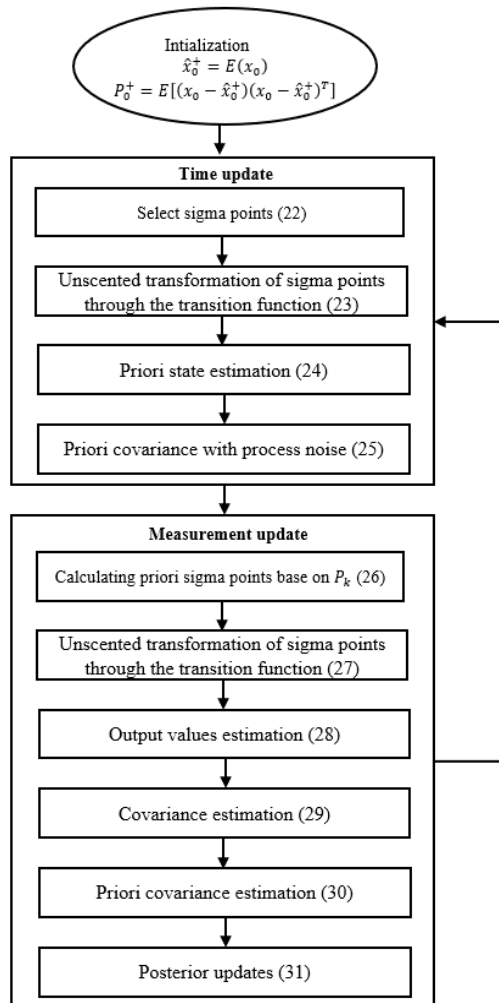


Figure 3. The SOC estimation flowchart

**4. EXPERIMENTS AND VALIDATION**

**4.1. Experimental scenarios**

The goal of the experiment is to demonstrate the effectiveness of the proposed estimation algorithm. Identifying the parameters of the battery equivalent circuit in real-time (online identification) using the VFFRLS algorithm. The determination of online parameters only requires measuring the current and voltage of the battery during operation. When the parameter is collected at each time step, the updated model is used to estimate the SOC value using the UKF. The structure of the SOC estimation process is indicated in Figure 4. The experimental model is set up as in Figure 5. The subject of analysis is a typical 18650 LIB cell. The installation parameters are as in Table 1.

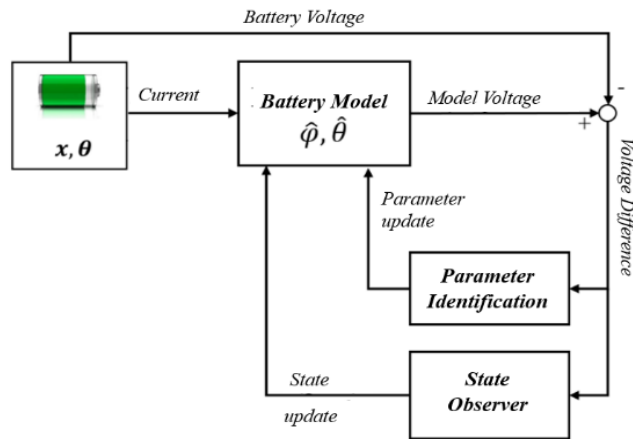


Figure 4. Structure of SOC estimation process

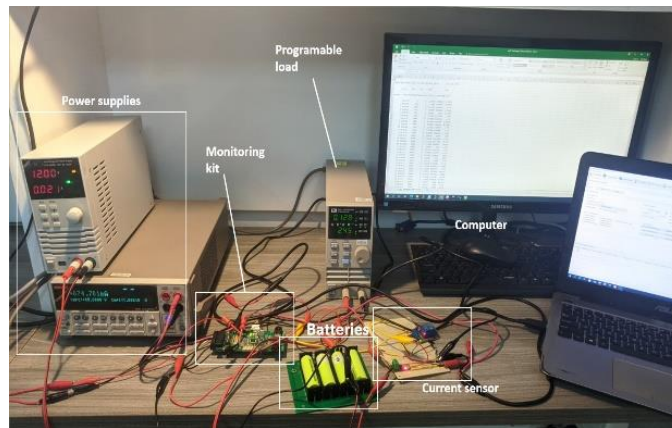


Figure 5. The experimental system model for SOC estimation

Table 1. Battery discharge/charging process information

Discharge process		Charging process	
Total discharge time	5500 s	Total charging time	8500 s
Discharge resistive load	2 $\Omega$	Constant current	2 A
Initial voltage (SOC=100%)	4.18 V	Initial voltage (SOC=20%)	3.4 V
End of cycle voltage (SOC=0%)	3.0 V	End of cycle voltage (SOC=100%)	4.19V
Connection time to load	100 s	Charger	ImaxB6

To achieve the above goal, the working condition of the battery is established in two cases: Discharge with constant resistive load as shown Figure 6(a) and CC-CV charging method as shown in Figure 6(b). The result of parameter identification is evaluated by comparing the voltage of the model output and the measured. SOC estimation results are evaluated by comparing them with the Coulomb counting method under experimental conditions.

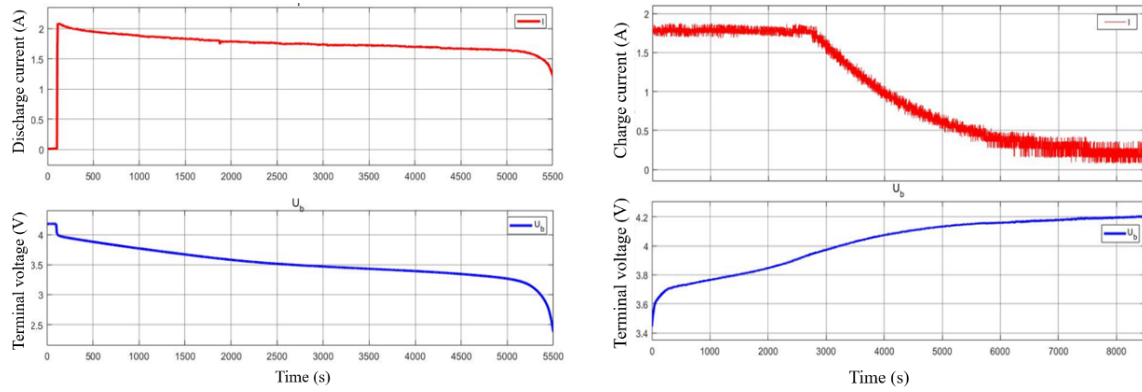


Figure 6. The current and voltage on the battery (a) discharging with constant resistive load and (b) charging with the CC-CV mode

**4.2. Parameter identification results**

Figure 7 shows the results of parameter identification during the discharging process. The OCV is also homogeneous and larger than the battery's 2-pole voltage. It is true in practice because the battery terminal voltage tends to increase when the load is disconnected. In addition, the internal resistance of the battery is about 80 mΩ in SOC is 100% and linearly reduces to 65 mΩ when SOC drops to 10%, at the last 10% of SOC, the resistance increases rapidly to 80 mΩ. Figure 8 shows the results of parameter identification during the charging process. OCV is also homogeneous and lower than the battery's 2-pole voltage. The internal resistance during charging and discharging is consistent with the information in the datasheet battery.

For further evaluation of parameter identification results, the voltage of the model output and measured are compared. Figures 9 and 10 show the voltage of the model output and measure during discharging/charging. The results indicate that the estimated voltage converges to the measured voltage for 10 seconds after connecting the load. This verifies the rapid convergence of the model as soon as the battery switches from a resting state to an active state. Errors in model output voltage and measurement voltage are assessed in Table 2 and Table 3.

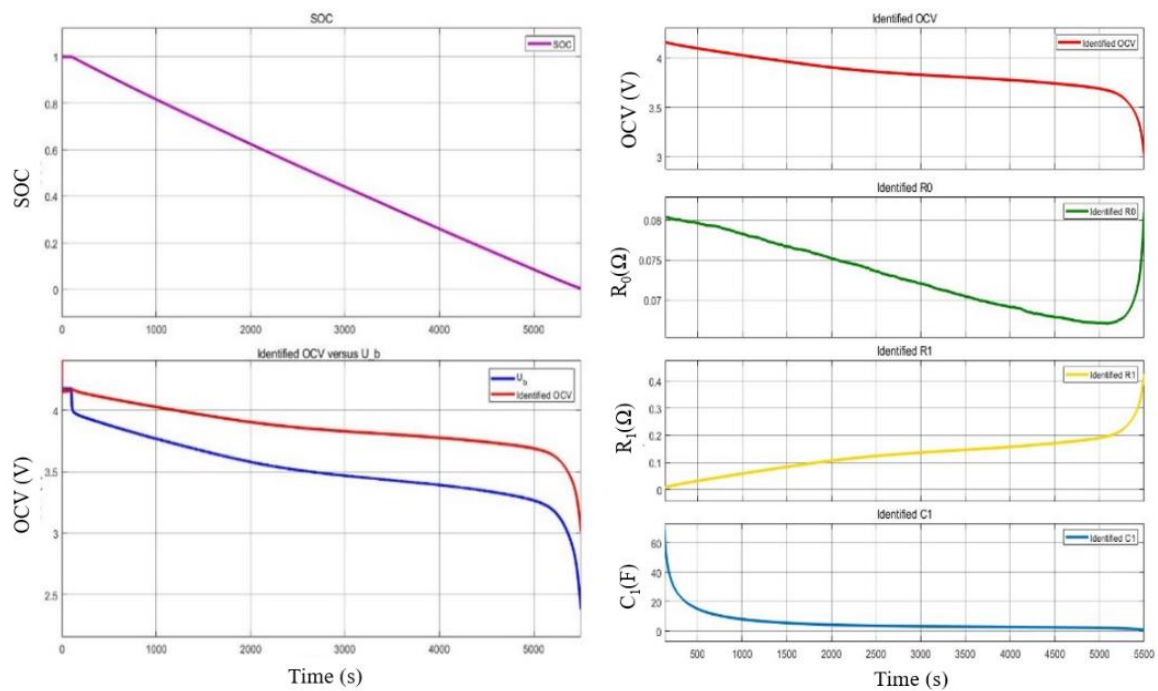


Figure 7. Battery model parameters identification during discharging

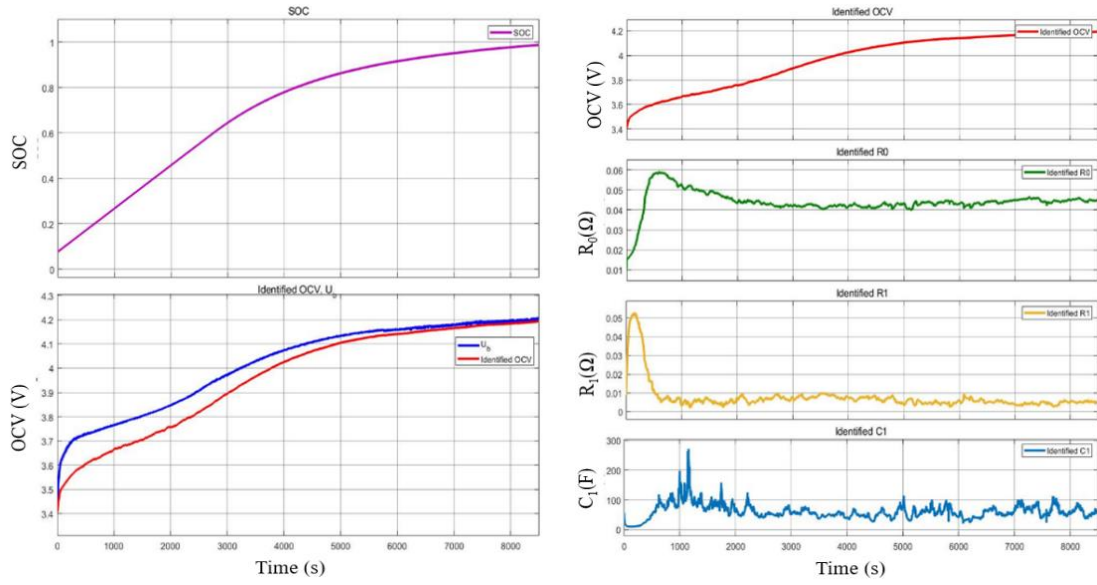


Figure 8. Battery model parameters identification during charging

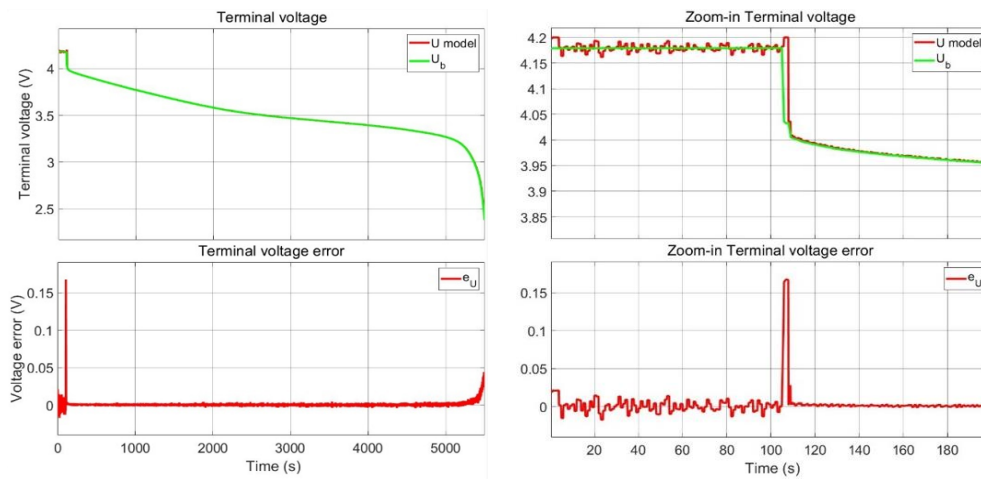


Figure 9. The voltage of model output and measure during discharging

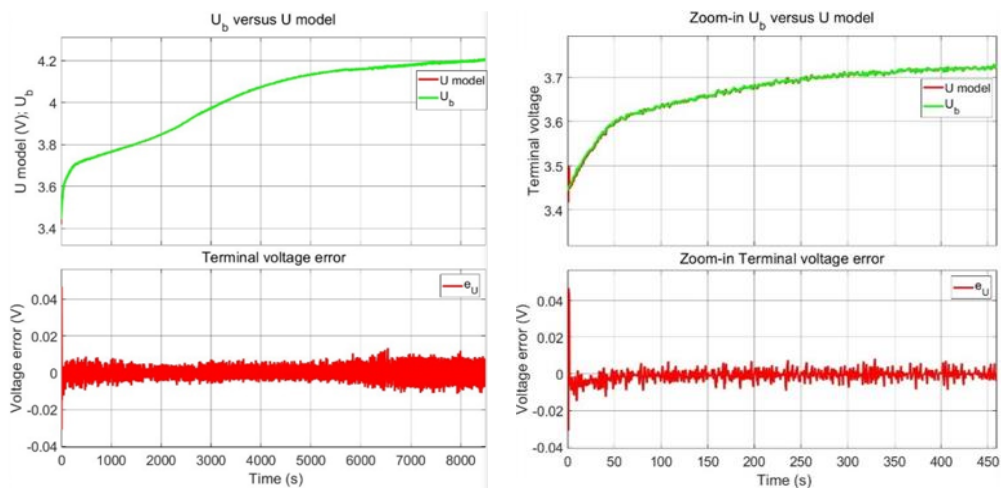


Figure 10. The voltage of model output and measure during charging

Table 2. Battery output voltage error during discharging

	Voltage error (mV)	
	MAE	RMSE
Overall	1.653	4.794
Before connecting to the load	9.488	25.01
After connecting to the load	1.491	3.290

Table 3. Battery output voltage error during charging

	Voltage error (mV)	
	MAE	RMSE
Overall	1.272	1.982
Constant current charging process	1.203	1.983
Constant voltage charging process	1.311	1.982

**4.3. SOC estimate by UKF**

The SOC estimated value of the VFFRLS-UKF proposed algorithm is compared with the Coulomb counting, the results of which not only demonstrate that UKF performs well under different noise uncertainties in measurements, but also verify that the model parameters are well identified. Figures 11 and 12 present the SOC estimation results during discharge and charge, respectively. The SOC estimation results obtained through the UKF algorithm show an over-adjustment time of 15 seconds and an error rate of less than 1%. Additionally, the static error drops to zero after 100 seconds.

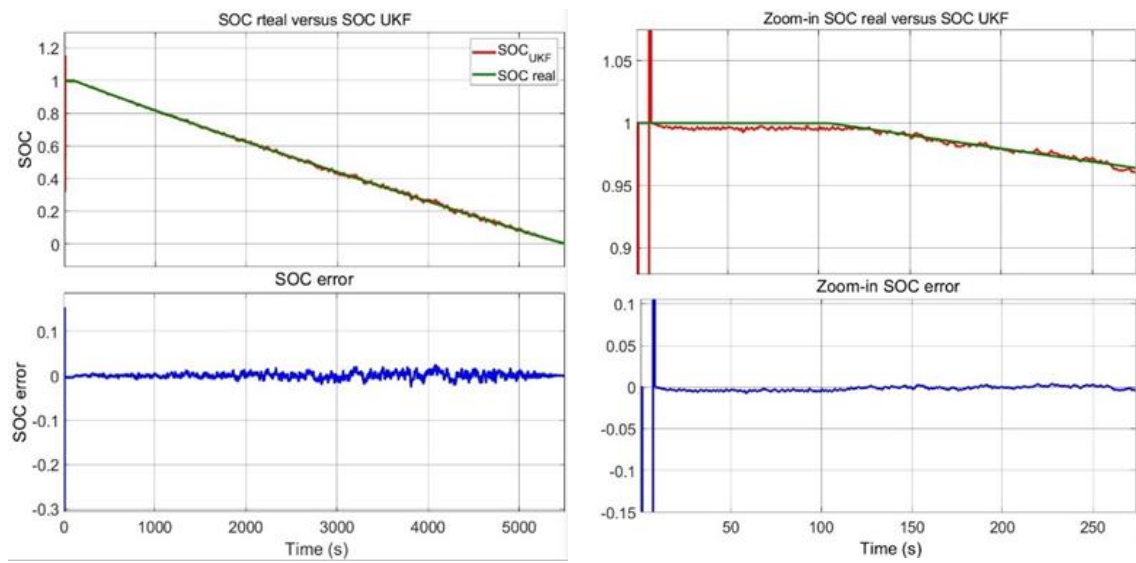


Figure 11. SOC estimation during discharging

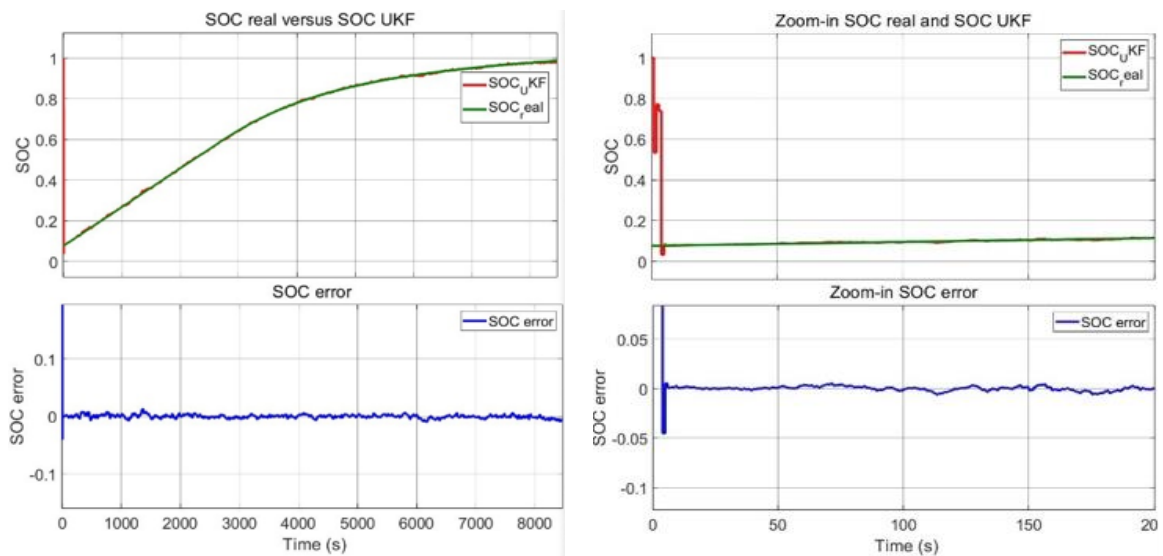


Figure 12. SOC estimation during charging

Table 4. SOC estimation errors during the discharging

Noise level	SOC error	
	MAE	RMSE
0	$1.995 \times 10^{-3}$	$2.864 \times 10^{-2}$
$1 \times 10^{-5}$	$1.932 \times 10^{-3}$	$2.713 \times 10^{-2}$
$1 \times 10^{-4}$	$2.846 \times 10^{-3}$	$2.626 \times 10^{-2}$
$1 \times 10^{-3}$	$5.366 \times 10^{-3}$	$1.853 \times 10^{-2}$
$1 \times 10^{-2}$	$8.481 \times 10^{-3}$	$1.445 \times 10^{-2}$

Table 5. SOC estimation errors during charging

Noise level	SOC error (CC-CV)	
	MAE	RMSE
0	$7.840 \times 10^{-4}$	$1.580 \times 10^{-2}$
$1 \times 10^{-5}$	$8.008 \times 10^{-4}$	$1.583 \times 10^{-2}$
$1 \times 10^{-4}$	$1.096 \times 10^{-3}$	$1.558 \times 10^{-2}$
$1 \times 10^{-3}$	$1.240 \times 10^{-3}$	$1.568 \times 10^{-2}$
$1 \times 10^{-2}$	$2.886 \times 10^{-3}$	$1.564 \times 10^{-2}$

By adding noise into the measurement data of current and voltage on the battery through MATLAB/Simulink simulation model, the effect of different noise characteristics is considered. The white gaussian noise was used with different power spectral density (PSD). The results of SOC estimation using the UKF during the discharging and charging cycles are presented in Tables 4 and 5, respectively.

#### 4.4. Comments and comparisons

##### 4.4.1. Parameter identification

Wei *et al.* [28] used an offline parameter determination method with the least squares algorithm generated errors of about 10 mV (MAE) but the estimated speed was slow. In [29] recursive least squares algorithm with a fixed forgetting factor is used to identify the parameters of one cell battery model with the model voltage error compared with voltages measured during a fixed current discharge of 37.6 mV (MAE) and 5.9 mV (RMSE), Ali *et al.* [30] achieved voltage errors of around 18.9 mV (MAE) and Rahimi-Eichi *et al.* [31] with moving window LS of about 16 mV (MAE). Meanwhile, VFFRLS presented in this paper voltage model errors and measuring voltages of only 1.653 mV (MAE) and 4.794 mV (RMSE) during discharge and 1.272 mV (MAE) and 1.982 mV (RMSE) during charging in Tables 2 and 3.

##### 4.4.2. SOC estimation

UKF observer used in the article gives good results. Specifically, VFFRLS-UKF gives SOC estimates errors of 0.19% (MAE) and 1.5% (RMSE) compared with the RLS-UKF method mentioned in [32] with 1.52% (MAE) and 1.52% (MAE) and 1.5% (RMSE) 1.8% (RMSE). The results of the proposed method were also significantly better than the results in [30] with 6% SOC error and 30 seconds convergence time. Comparing the two stages of the proposed method we can see VFFRLS-UKF in the paper gives good estimated results compared to the overall studies that went before and converged in a shorter period.

## 5. CONCLUSION

The online SOC estimation method using the VFFRLS-UKF algorithm proposed in this paper has high accuracy. Specifically, the VFFRLS parameter identification algorithm has given the ability to effectively initialize the physical parameters of the model with an output voltage error of less than 0.1% of the nominal voltage. Besides, the UKF filter provides the results with a 1.5% error from the reference and converges after 10 cycles. These are acceptable results, confirming the accurate estimate ability of UKF and parameter identification. As such, the proposed method of combining online parameter identification and state observer using UKF shows high efficiency in SOC estimation of the nonlinear system such as Lithium-ion battery that other state observers difficult to achieve.

## REFERENCES

- [1] J. A. Sanguesa, V. Torres-Sanz, P. Garrido, F. J. Martinez, and J. M. Marquez-Barja, "A review on electric vehicles: technologies and challenges," *Smart Cities*, vol. 4, no. 1, pp. 372–404, Mar. 2021, doi: 10.3390/smartcities4010022.
- [2] M. A. Xavier and M. S. Trimboli, "Lithium-ion battery cell-level control using constrained model predictive control and equivalent circuit models," *Journal of Power Sources*, vol. 285, pp. 374–384, Jul. 2015, doi: 10.1016/j.jpowsour.2015.03.074.
- [3] M. A. Hannan, M. S. H. Lipu, A. Hussain, and A. Mohamed, "A review of lithium-ion battery state of charge estimation and management system in electric vehicle applications: Challenges and recommendations," *Renewable and Sustainable Energy*

- Reviews*, vol. 78, pp. 834–854, Oct. 2017, doi: 10.1016/j.rser.2017.05.001.
- [4] Y. Chen *et al.*, “A review of lithium-ion battery safety concerns: The issues, strategies, and testing standards,” *Journal of Energy Chemistry*, vol. 59, pp. 83–99, Aug. 2021, doi: 10.1016/j.jechem.2020.10.017.
  - [5] Z. Li, J. Huang, B. Y. Liaw, and J. Zhang, “On state-of-charge determination for lithium-ion batteries,” *Journal of Power Sources*, vol. 348, pp. 281–301, Apr. 2017, doi: 10.1016/j.jpowsour.2017.03.001.
  - [6] M. S. H. Lipu *et al.*, “Battery management, key technologies, methods, issues, and future trends of electric vehicles: a pathway toward achieving sustainable development goals,” *Batteries*, vol. 8, no. 9, Sep. 2022, doi: 10.3390/batteries8090119.
  - [7] A. M. S. M. H. S. Attanayaka, J. P. Karunadasa, and K. T. M. U. Hemapala, “Estimation of state of charge for lithium-ion batteries - a review,” *AIMS Energy*, vol. 7, no. 2, pp. 186–210, 2019, doi: 10.3934/ENERGY.2019.2.186.
  - [8] I. B. Espedal, A. Jinasena, O. S. Burheim, and J. J. Lamb, “Current trends for state-of-charge (SoC) estimation in lithium-ion battery electric vehicles,” *Energies*, vol. 14, no. 11, Jun. 2021, doi: 10.3390/en14113284.
  - [9] X. Hu, F. Feng, K. Liu, L. Zhang, J. Xie, and B. Liu, “State estimation for advanced battery management: Key challenges and future trends,” *Renewable and Sustainable Energy Reviews*, vol. 114, Oct. 2019, doi: 10.1016/j.rser.2019.109334.
  - [10] M. U. Ali, A. Zafar, S. H. Nengroo, S. Hussain, M. J. Alvi, and H. J. Kim, “Towards a smarter battery management system for electric vehicle applications: a critical review of lithium-ion battery state of charge estimation,” *Energies*, vol. 12, no. 3, Jan. 2019, doi: 10.3390/en12030446.
  - [11] R. Zhang *et al.*, “State of the art of lithium-ion battery SOC estimation for electrical vehicles,” *Energies*, vol. 11, no. 7, Jul. 2018, doi: 10.3390/en11071820.
  - [12] K. Movassagh, A. Raihan, B. Balasingam, and K. Pattipati, “A critical look at coulomb counting approach for state of charge estimation in batteries,” *Energies*, vol. 14, no. 14, Jul. 2021, doi: 10.3390/en14144074.
  - [13] E. Chemali, P. J. Kollmeyer, M. Preindl, and A. Emadi, “State-of-charge estimation of Li-ion batteries using deep neural networks: A machine learning approach,” *Journal of Power Sources*, vol. 400, pp. 242–255, Oct. 2018, doi: 10.1016/j.jpowsour.2018.06.104.
  - [14] L. Ma, C. Hu, and F. Cheng, “State of charge and state of energy estimation for Lithium-Ion batteries based on a long short-term memory neural network,” *Journal of Energy Storage*, vol. 37, May 2021, doi: 10.1016/j.est.2021.102440.
  - [15] A. Azwan, A. Razak, M. F. M. Jusof, A. N. K. Nasir, and M. A. Ahmad, “A multiobjective simulated Kalman filter optimization algorithm,” in *Proceedings of 4th IEEE International Conference on Applied System Innovation 2018, ICASI 2018*, Apr. 2018, pp. 23–26, doi: 10.1109/ICASI.2018.8394257.
  - [16] P. Takyi-Aninakwa, S. Wang, H. Zhang, E. Appiah, E. D. Bobobee, and C. Fernandez, “A strong tracking adaptive fading-extended Kalman filter for the state of charge estimation of lithium-ion batteries,” *International Journal of Energy Research*, vol. 46, no. 12, pp. 16427–16444, Jun. 2022, doi: 10.1002/er.8307.
  - [17] M. F. M. Jusof *et al.*, “A Kalman-filter-based sine-cosine algorithm,” in *2018 IEEE International Conference on Automatic Control and Intelligent Systems (I2CACIS)*, Oct. 2018, pp. 137–141, doi: 10.1109/I2CACIS.2018.8603711.
  - [18] J. Khodaparast, “A review of dynamic phasor estimation by non-linear Kalman filters,” *IEEE Access*, vol. 10, pp. 11090–11109, 2022, doi: 10.1109/ACCESS.2022.3146732.
  - [19] Z. Zhang, L. Jiang, L. Zhang, and C. Huang, “State-of-charge estimation of Lithium-Ion battery pack by using an adaptive extended Kalman filter for electric vehicles,” *Journal of Energy Storage*, vol. 37, May 2021, doi: 10.1016/j.est.2021.102457.
  - [20] Y. Chen, D. Huang, Q. Zhu, W. Liu, C. Liu, and N. Xiong, “Article a new state of charge estimation algorithm for lithium-ion batteries based on the fractional unscented kalman filter,” *Energies*, vol. 10, no. 9, Sep. 2017, doi: 10.3390/en10091313.
  - [21] X. Wu, X. Li, and J. Du, “State of charge estimation of Lithium-Ion batteries over wide temperature range using unscented Kalman filter,” *IEEE Access*, vol. 6, pp. 41993–42003, 2018, doi: 10.1109/ACCESS.2018.2860050.
  - [22] P. Zhang, C. Xie, and S. Dong, “State of charge estimation of lithium battery based on dual adaptive unscented Kalman filter,” in *2018 IEEE International Power Electronics and Application Conference and Exposition (PEAC)*, Nov. 2018, pp. 1–6, doi: 10.1109/PEAC.2018.8590470.
  - [23] M. Shehab El Din, A. A. Hussein, and M. F. Abdel-Hafez, “Improved battery SOC estimation accuracy using a modified UKF with an adaptive cell model under real EV operating conditions,” *IEEE Transactions on Transportation Electrification*, vol. 4, no. 2, pp. 408–417, Jun. 2018, doi: 10.1109/TTE.2018.2802043.
  - [24] C. Weng, J. Sun, and H. Peng, “A unified open-circuit-voltage model of lithium-ion batteries for state-of-charge estimation and state-of-health monitoring,” *Journal of Power Sources*, vol. 258, pp. 228–237, Jul. 2014, doi: 10.1016/j.jpowsour.2014.02.026.
  - [25] Q. Yu, R. Xiong, and C. Lin, “Online estimation of state-of-charge based on the H infinity and unscented kalman filters for Lithium Ion batteries,” *Energy Procedia*, vol. 105, pp. 2791–2796, May 2017, doi: 10.1016/j.egypro.2017.03.600.
  - [26] M. Dubarry and B. Y. Liaw, “Development of a universal modeling tool for rechargeable lithium batteries,” *Journal of Power Sources*, vol. 174, no. 2, pp. 856–860, Dec. 2007, doi: 10.1016/j.jpowsour.2007.06.157.
  - [27] N. K. Trung and N. T. Diep, “Online parameter identification for equivalent circuit model of lithium-ion battery,” *Indonesian Journal of Electrical Engineering and Computer Science (IJECS)*, vol. 31, no. 1, pp. 151–159, Jul. 2023, doi: 10.11591/ijeecs.v31.i1.pp151-159.
  - [28] Z. Wei, D. Zhao, H. He, W. Cao, and G. Dong, “A noise-tolerant model parameterization method for lithium-ion battery management system,” *Applied Energy*, vol. 268, Jun. 2020, doi: 10.1016/j.apenergy.2020.114932.
  - [29] X. Zhang, Y. Wang, D. Yang, and Z. Chen, “An on-line estimation of battery pack parameters and state-of-charge using dual filters based on pack model,” *Energy*, vol. 115, pp. 219–229, Nov. 2016, doi: 10.1016/j.energy.2016.08.109.
  - [30] D. Ali, S. Mukhopadhyay, H. Rehman, and A. Khurram, “UAS based Li-ion battery model parameters estimation,” *Control Engineering Practice*, vol. 66, pp. 126–145, Sep. 2017, doi: 10.1016/j.conengprac.2017.06.012.
  - [31] H. Rahimi-Eichi, F. Baronti, and M. Y. Chow, “Online adaptive parameter identification and state-of-charge coestimation for lithium-polymer battery cells,” *IEEE Transactions on Industrial Electronics*, vol. 61, no. 4, pp. 2053–2061, Apr. 2014, doi: 10.1109/TIE.2013.2263774.
  - [32] Z. Wei, G. Dong, X. Zhang, J. Pou, Z. Quan, and H. He, “Noise-immune model identification and state-of-charge estimation for Lithium-Ion battery using bilinear parameterization,” *IEEE Transactions on Industrial Electronics*, vol. 68, no. 1, pp. 312–323, Jan. 2021, doi: 10.1109/TIE.2019.2962429.

**BIOGRAPHIES OF AUTHORS**

**Nguyen Thi Diep**     received a Ph.D degree in control and automation from the Hanoi University of Science and Technology, Hanoi, Vietnam in 2021. She is currently working as a Lecturer at Electric Power University, Hanoi, Vietnam. Her current research includes high-frequency converters, battery charging technology for EVs, and wireless power transfer systems. She can be contacted at email: [diepnt@epu.edu.vn](mailto:diepnt@epu.edu.vn).



**Nguyen Kien Trung**     was born in Hanoi, Vietnam. He received the B.E. and M.Sc. degrees in control and automation from Hanoi University of Science and Technology, Vietnam in 2008 and 2011, respectively. In 2016, he received a Ph.D. degree in functional control systems at Shibaura Institute of Technology, Japan, where he worked as a postdoctoral researcher from 2016-2017. In 2008, he joined the Department of Industrial Automation, at Hanoi University of Science and Technology. Dr. Trung is a member of the IEEE and IEE of Japan. His current research interests include high-frequency converters, Battery charging technology for EVs, battery management systems, and wireless power transfer systems. He can be contacted at email: [trung.nguyenkien1@hust.edu.vn](mailto:trung.nguyenkien1@hust.edu.vn).